Surface Science 677 (2018) 296–300

Contents lists available at ScienceDirect

Surface Science

journal homepage: www.elsevier.com/locate/susc

The effect of single pd atoms on the energetics of recombinative O_2 desorption from Au(111)

Felicia R. Lucci[a], Liang Zhang[b], Theodore Thuening[a], Matthew B. Uhlman[a], Alex C. Schilling[a], Graeme Henkelman[b], E. Charles H. Sykes[a,*]

[a] Department of Chemistry, Tufts University, 62 Talbot Ave., Medford, MA 02155, USA
[b] Department of Chemistry and the Institute for Computational and Engineering Sciences, University of Texas at Austin, Austin, TX 78712, USA

ABSTRACT

The oxidation of gold is an important step in a number of catalytic reactions and the oxidation of Au(111) with ozone has been well-studied using surface science techniques. We report that the addition of 1% Pd in the surface in the form of a Pd/Au(111) single-atom alloy dramatically alters the desorption temperature of molecular oxygen after oxidation by ozone. We use temperature programmed desorption to study the desorption kinetics and scanning tunneling microscopy to compare the structure of the oxides produced on Au(111) with and without 1% Pd. Aided by density functional theory we hypothesize that the lower temperature evolution of O_2 occurs not because Pd atoms lower the O_2 desorption barrier, rather than the 1% Pd disrupts the formation of the more stable 2D ordered oxide formed on Au(11). This effect is particularly pronounced when the single-atom alloy surface is treated with ozone at lower temperatures.

1. Introduction

Heterogeneous catalysts that utilize isolated metal atoms are emerging as a promising approach for the efficient use of precious metal catalysts to enhance catalytic activity [1,2]. Both bimetallic *single-atom alloys* and oxide supported single atoms have been shown to catalyze numerous reactions including water gas shift [3,4], hydrogenation [5–10], dehydrogenation [11], oxidation [12,13], hydrogenolysis [14], and coupling reactions [15]. However, direct investigation of isolated atoms in real catalysts is often difficult due to the complexity of the catalyst structure. Recently, we developed the single-atom alloy (SAA) approach for catalyst design where we initially studied the structure and chemistry of isolated atoms in single crystal model catalysts [16–20]. Over the years this work has informed the design of nanoparticle catalysts capable of catalyzing selective hydrogenation reactions with improved tolerance to CO poisoning under realistic operating pressures as well as C—H activation chemistry [18,19]. We were curious to investigate if single atoms had any effect on oxygen surface chemistry, and in this study we probe the adsorption and desorption of oxygen from isolated Pd monomers in a Au(111) substrate.

Au nanoparticles and nanoporous Au are well known for highly selective oxidation reactions despite the high barrier for O_2 activation on Au [21–26]. The addition of Pd to Au catalysts increases the reactivity of Au and this alloy combination exhibits remarkable selectivity for catalyzing CO oxidation [3], vinyl acetate synthesis [27–29], alcohol oxidation [30], and hydrogen peroxide synthesis [31]. In these reactions, the atomic ensemble of the Pd atoms in Au is critical to obtain the desired selectivity. It has been shown for CO oxidation that contiguous Pd atoms are necessary for O_2 activation [32] and for vinyl acetate synthesis Pd monomers prevent the unwanted oxidation of products [27,29]. Despite the importance of the above reactions, the fundamental interaction between O and isolated Pd atoms in Au is not well understood. Previous studies by Li et al. and Yu et al. show extended Pd sites are required for the dissociative adsorption of O_2 on Au-Pd(100) [33] and Pd-Au(111) [34], respectively. In both studies a dramatic decrease in O_2 uptake was observed at low concentrations of surface Pd atoms, suggesting a geometric ensemble effect for the adsorption and dissociation of O_2. Neither study, however, experimentally probed the capabilities of isolated metal geometries. In the current work, we directly addressed the effects of single Pd atom geometries on the recombinative desorption of O_2 from Au(111). Since Au(111) is unable to dissociate O_2 in ultra-high vacuum (UHV), we used ozone to populate the surfaces with O.

By using a combination of temperature programmed desorption, scanning tunneling microscopy, and density function theory, we probed the impact of 1% isolated Pd atoms on how oxygen interacts with a Au (111) surface. Our studies reveal that these small amounts of Pd lead to a significant reduction in the O_2 desorption temperature at low O coverages. Our DFT calculations reveal that isolated Pd monomers in Au(111) in fact increase the barrier for dissociative adsorption of O_2 and the barrier for recombinative desorption of O_2 very slightly. Our STM results show that 1% single Pd atoms prevent the formation of the

* Corresponding author.
E-mail address: charles.sykes@tufts.edu (E. Charles H. Sykes).

https://doi.org/10.1016/j.susc.2018.08.001
Received 21 June 2018; Received in revised form 27 July 2018; Accepted 2 August 2018
Available online 08 August 2018
0039-6028/

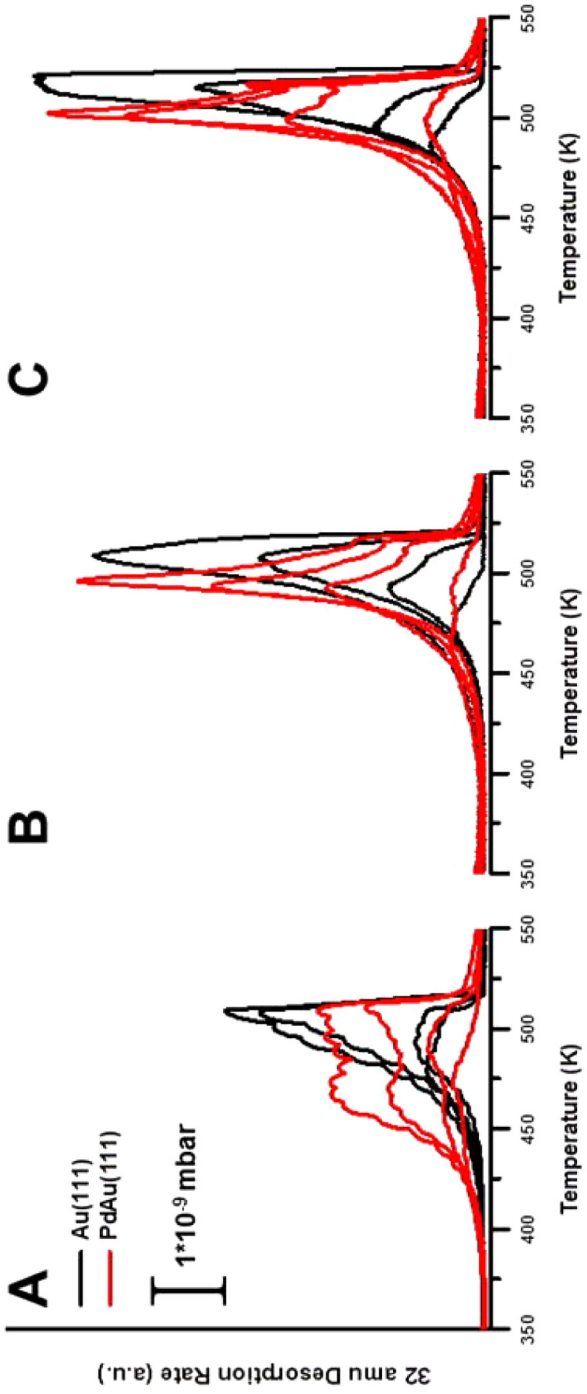

Fig. 1. TPD traces for O_2 desorption from Au(111) and 1% (0.01 ML) PdAu(111) SAAs after a series of low temperature ozone exposures at (A) 85 K and high temperature ozone exposures at (B) 290 K and (C) 400 K (y scale is consistent for all).

2D Au surface oxide from which O_2 is known to desorb in a decomposition rate limited process [35]. Since disordered oxygen on Au(111) at low coverage is known to be more reactive than both, bare Au(111) [36,37] and oxygen on Au(111) at high coverages [38], we speculate that small amounts of Pd, or other elements like Ni, may alter the initial oxidation of Au, allow it to desorb at lower temperature, and hence be used to control the subsequent reactivity of the system.

2. Materials and methods

Imaging and thermal desorption analysis were performed in separate ultra-high vacuum chambers (base pressures $<1 \times 10^{-10}$ mbar) on two Au(111) single crystals cleaned by successive cycles of Ar + sputtering (1.5 keV, 20 μA) followed by annealing to 720 K. Cleanliness was monitored via STM imaging and XPS. Palladium was deposited on the Au single crystal in vacuo by physical vapor deposition (EFM 3, Focus GmbH) where the flux of Pd was set to 0.01 ML/min and the sample was held at 380 K during the entire deposition process. 1% Pd single-atom alloy surfaces were confirmed by STM characterization as well as by CO TPD as described previously [39]. Ozone was produced from an LG-7 ozone generator (Del Ozone) from O_2 (99.994%, Airgas) and was dosed to the prepared surfaces through a variable leak valve utilizing a linear collimator in order to enhance ozone pressure localized at the sample surface. The TPD traces were all produced by depositing ozone on the surface at a pressure of 5×10^{-7} mbar for various exposure times between 1 minute and 30 minutes. STM images were collected using a variable temperature STM (Omicron Nano-Technology) at 290 K and 30 K. TPD spectra were collected, at a heating rate of 1 K/s, in a chamber equipped with a quadrupole mass spectrometer (HAL 301, Hiden Analytical) with the ability to cool to 80 K.

3. Theory

Density functional theory (DFT) was used to calculate all energetics, using the Vienna *ab initio* simulation package [40,41]. Core electrons were described using the projector-augmented wave method [42,43]. Kohn-Sham single-electron wave functions were expanded in a plane-wave basis with a kinetic energy cutoff of 300 eV to describe the valence electrons. The Perdew – Burke – Ernzerhof (PBE) generalized gradient approximation functional was used to describe the exchange correlation contribution to the total energy [44]. Geometries were considered optimized when the force on each atom was < 0.01 eV/Å. All the transition states were calculated with the climbing-image nudged elastic band method (CI-NEB) [45,46].

A four-layer 4 × 4 Au(111) slab is used to model the Au surface with the bottom two layers fixed to bulk Au positions. The Pd_1-Au(111) surface in this study was modeled by replacing one Au atoms on the top layer of the Au(111) slab with Pd. A 10 Å vacuum was added to all models to avoid interactions between periodic images. The Brillouin zone was sampled using a 3 × 3 × 1 Monkhorst – Pack k-point mesh [47].

4. Results and discussion

The 1% PdAu *single-atom alloy* surface morphology was characterized using STM (Figure S1) and has also been well described in the literature [48–57]. Briefly, at low Pd coverages, Pd atoms exist as isolated atoms in the Au surface due to stronger hetero-atom bonds between Pd-Au than Pd-Pd or Au-Au (Figure S1B). During the place exchange of Pd atoms into the Au terraces, Au adatoms are ejected and nucleate into islands on the surface (Figure S1A). The surface layer of the islands are primarily composed of Au atoms due to the lower surface free energy of Au than Pd. Due to the large activation barrier of O_2 dissociative adsorption onto Au(111), it is not possible to adsorb O onto the Au(111) surface in UHV from molecular oxygen. Thus, for these experiments, O was adsorbed onto Au(111) and Pd/Au(111) SAA by

exposure of the surface to ozone as reported previously [58,59].

Significant differences in O_2 desorption are observed with TPD between Au(111) and PdAu(111) alloys. After exposure of Au(111) to ozone at 85 K, low coverages of O_2 were observed desorbing at 510 K (Fig. 1A) in reasonable agreement with low oxygen coverages in previously reported work [58,60–63]. The desorption profiles of O_2 from Au(111) do not follow typical second order desorption trends suggesting the simple recombination of 2 O adatoms is not the rate limiting step. Work by Koel [58] and Friend [60] has shown that, independent of coverage, the desorption order of O_2 from Au(111) is 1, with the rate limiting step believed to be the decomposition of the a 2D surface oxide followed by subsequent recombination and desorption. It has been previously reported that O surface coverage on Au(111) saturates at 1.2 ML when exposed to ozone at room temperature [58]. Since our O_2 desorption peaks do not saturate, our surface coverages are below 1 ML due to a low flux of incoming O_3 molecules in our experimental setup. For the PdAu(111) SAA with ozone dosed at 85 K, O_2 desorbs at 470 K for low O coverages. At higher O coverages, a second desorption peak was observed at 510 K corresponding to desorption from the Au(111) surface. Thus, the isolated Pd atoms open a distinct low temperature O_2 desorption pathway from the surface. One must also consider if the Au islands formed from the Au atoms ejected by the Pd atoms could lead to the low temperature oxygen desorption we observe. However, we think this is unlikely because only 1% Pd is added to the surface which means at most 1% of the surface would be covered by ejected Au atom islands. Since the Au(111) surface already has a similar amount of defects in the form of step edges (typically step edge density on pristine Au(111) is 1–2%), and the oxide forms an ordered structure on the bare Au(111), it appears that the cause of the disordered oxide is the single Pd atoms.

To determine the morphology of the surface during the initial stages of oxidation at low temperatures a Au(111) surface oxidized at 110 K was imaged with STM. The STM images show dark amorphous depressions in registry with the Au herringbone reconstruction (Fig. 2A and inset). Our images also show that oxidation is inhomogeneous; dark oxide patches emanate from a defect created in the very first stage of oxidation (lower middle of Fig. 2A). Previously, it has been shown that surface oxides appear darker than the surrounding metallic surface in STM images [64]. Localized regions of pits are also observed to be ~390 pm deep which is greater than an atomic layer of Au (235 pm), suggesting the pits are composed of an oxidized state of Au. For PdAu (111) SAAs exposed to ozone, we do not observe localized oxide patches, rather much more disordered surface structures with small islands that may be caused by the removal of Au and Pd atoms by oxygen (Fig. 2B). For the Pd/Au SAA, the amorphous depressions in registry with the Au herringbone pattern were present similar to the Au(111).

To further investigate the effect of Pd on oxygen desorption from Au (111) we exposed both Au(111) and Pd/Au SAA surfaces to ozone at elevated temperatures in accordance with previous studies which have shown different oxide structures depending on ozone exposure temperature [59]. Resulting TPD and STM data for ozone exposure at 290 K are displayed in Figs. 1B and 3 respectively. As with ozone exposure at 85 K, one desorption state (centered at ~510 K) dominates on bare Au (111). With the addition of Pd single atoms a lower temperature desorption pathway is again observed, but with a decrease in the difference in desorption temperatures (now ~25 K) from PdAu SAA sites and Au (111)-like sites. Two distinct states were observed with STM including ordered oxide islands that form row like structures on the bare Au(111) surface, (Fig. 3A) vs. an amorphous oxide structure on the partially oxidized PdAu SAA surface (Fig. 3B). The STM results again suggest that 1% Pd atoms alter the structure of the oxide which is consistent with the low temperature desorption observed for O_2 from PdAu SAAs (Fig. 1B). Specifically, the ordered 2D oxide formed on pure Au(111) requires higher temperatures to decompose [58,60] while the disordered oxide formed on PdAu SAAs is able to decompose at lower temperatures compared to the bare surface as observed via TPD. Following this trend, ozone exposure at 400 K (Fig. 1C) displays a peak temperature of ~520 K on Au(111) with the lower temperature, PdAu SAA O_2 desorption peak at ~500 K (now only 20 K lower than from Au (111)). It is important to note that even at an ozone exposure temperature of 400 K, the O_2 desorption peak continues to broaden but does not saturate (Fig. 1C).

In order to examine both the adsorption and desorption kinetics of O_2, we calculated the activation energy for dissociative adsorption and desorption energy for the recombinative desorption of O_2 with DFT (Fig. 4). The recombinative desorption barrier of O_2 from a Pd/Au SAA (1.28 eV) is slightly higher than the recombinative desorption barrier from bare Au(111) (1.27 eV) however this 0.01 eV difference is within the error of DFT so it would not be expected that any difference in O_2 desorption temperature would be observed if recombination of two O atoms was the rate limiting step in desorption. The 40 K decrease in desorption temperature from Pd/Au(111) SAAs compared to Au(111) observed experimentally must instead be due to another effect. According to Redhead analysis for a first order desorption process assuming a pre-exponential of 1×10^{15}, the difference in desorption barriers for desorption from Au(111) (510 K, 1.64 eV) and Pd-Au(111) SAAs (470 K, 1.51 eV) should be ~0.1 eV. The DFT results provide an activation energy for dissociative O_2 adsorption of 0.19 eV larger for Pd/Au(111) than Au(111) since O_2 physisorption is stronger on Pd/Au SAAs than pure on Au(111). As a result the dissociative adsorption barrier is larger for Pd/Au SAAs than Au(111) which is certainly non-intuitive as Pd is typically more active than Au. This supports previous work on Pd/Au(111) [34] and Au/Pd(100) [33] which suggest isolated Pd atoms cannot activate O_2. These studies report low temperature physisorption of O_2 on extended Pd ensembles where the adsorbed coverage of O_2 is dependent on the surface concentration of Pd. Both studies report a non-linear decrease in O_2 uptake as a function of Pd coverage suggesting that geometric ensemble effects impact the physisorption of O_2 and sequential dissociation to adsorbed O atoms.

In summary, our TPD data reveal a distinct low temperature O_2 desorption state upon sub-monolayer exposure of ozone after

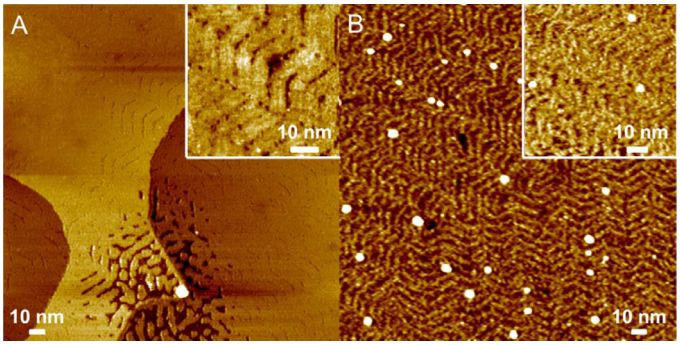

Fig. 2. STM images of (A) Au(111) and (B) 1% PdAu(111) SAAs oxidized at 110 K. (A) Large scale image shows both depressions in registry with the herringbone reconstruction (inset) and oxidation pits. (B) Large scale and local (inset) disruption in ordered oxide structures with 1% Pd SAAs.

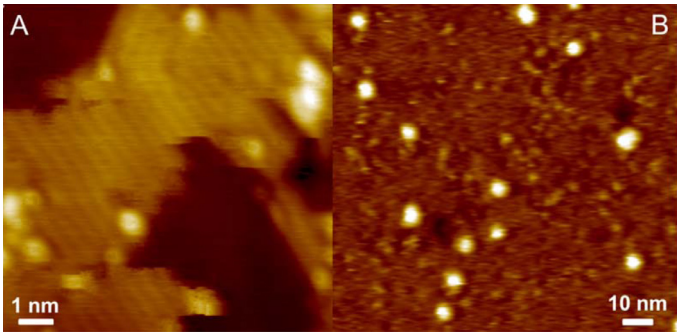

Fig. 3. STM images of (A) Au(111) and (B) PdAu(111) SAAs oxidized at 290 K. (A) Image shows ordered oxide islands. (B) Large scale disordered surface with 1% Pd SAAs.

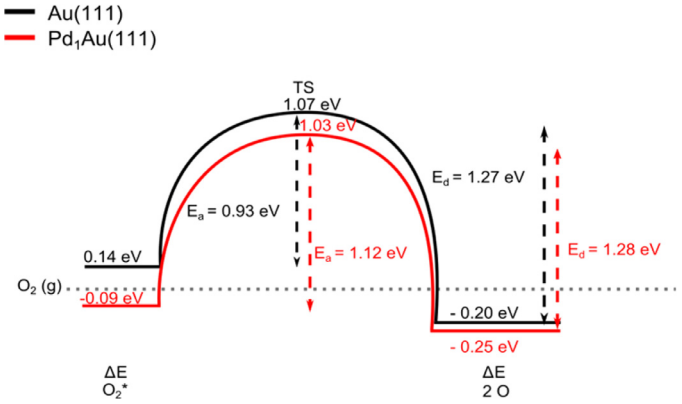

Fig. 4. DFT calculated energy landscape for O_2 adsorption and desorption from Au and Pd-Au SAAs. Shown are adsorption energies (ΔE) of O_2 (0.14 eV and −0.09 eV) and 2 O (−0.20 eV and −0.25 eV), activation energy for dissociative adsorption of O_2 (E_a) and desorption energy for recombinative desorption of O_2 (E_d) for both Au and PdAu surfaces.

substitution of 1% Pd atoms dispersed in the Au(111) surface. STM results confirm a change in surface structure of the oxide by comparing images of the surface after ozone exposure with Pd single atoms present vs. the surface oxide on bare Au(111). It is unlikely the cause of this low temperature desorption feature is due to isolated Pd sites, as Pd dimers are required for facile O_2 recombinative desorption. Our DFT results agree, and in fact show that the barrier for O_2 desorption is very similar to the barrier for the bare Au(111) surface. These results, in concert with the general agreement in the literature for ozone adsorption on Au (111), point toward the 1% Pd single atoms disrupting the formation of a 2D gold oxide, which has been shown to be the rate limiting step in O_2 desorption from Au(111) surfaces. It would be interesting in future work on this system to explore if other dopant atoms also yielded the effect we report with Pd.

5. Conclusions

O_2 desorption from the 1% Pd/Au(111) SAAs exhibits a unique lower temperature desorption profile compared to Au(111). After ozone exposure at 85 K, O_2 desorbs at 470 K, 40 K lower than desorption from Au(111) (Fig. 1A). When the same Pd/Au SAA is exposed to ozone at 290 K and 400 K, O_2 desorption occurs at 490 K and continues to shift to higher temperatures with increasing O coverage. Our STM experiments show that an amorphous oxide surface structure is observed on the Pd/Au surface suggesting that the 1% Pd atoms prevent the formation of the 2D oxide. Therefore, we postulate that the low temperature desorption of O_2 from Pd-Au SAAs is due to the formation of the 2D oxide (decomposition of which is known to be the rate limiting step of O_2 desorption from Au(111)) being hindered by the presence of 1% Pd. The pronounced shift in O_2 desorption at low oxygen surface coverages suggests that Pd atoms locally affect oxide formation on Au as at higher oxygen coverages and deposition temperatures the peak centers are only ~20 K apart.

Acknowledgments

The work at Tufts was supported by the Department of Energy Basic Energy Sciences program under grant number DE-FG02-05ER15730. G.H. and L.Z. thanks the Welch Foundation (grant# F-1841).

Supplementary materials

Supplementary material associated with this article can be found, in the online version, at doi:10.1016/j.susc.2018.08.001.

References

[1] J.M. Thomas, Z. Saghi, P.L. Gai, Can a single atom serve as the active site in some heterogeneous catalysts? Top. Catal. 54 (2011) 588–594, https://doi.org/10.1007/s11244-011-9677-y.
[2] J.M. Thomas, The concept, reality and utility of single-site heterogeneous catalysts (SSHCs), Phys. Chem. Chem. Phys. 16 (2014) 7647–7661, https://doi.org/10.1039/c4cp00513a.
[3] Y. Zhai, D. Pierre, R. Si, W. Deng, P. Ferrin, A.U. Nilekar, G. Peng, J.A. Herron, D.C. Bell, H. Saltsburg, M. Mavrikakis, M. Flytzani-Stephanopoulos, Alkali-stabilized Pt-OHx species catalyze low-temperature water-gas shift reactions, Science 329 (2010) 1633–1636, https://doi.org/10.1126/science.1192449.
[4] Q. Fu, H. Saltsburg, M. Flytzani-Stephanopoulos, Active nonmetallic au and pt species on ceria-based water-gas shift catalysts, Science 301 (2003) 935–938, https://doi.org/10.1126/science.1085721.
[5] G. Vilé, D. Albani, M. Nachtegaal, Z. Chen, D. Dontsova, M. Antonietti, N. López, J. Pérez-Ramírez, A stable single-site palladium catalyst for hydrogenations, Angew. Chemie Int. Ed. 54 (2015) 11265–11269, https://doi.org/10.1002/anie.201505073.
[6] X. Zhang, H. Shi, B.-Q. Xu, Catalysis by gold: isolated surface Au3+ ions are active sites for selective hydrogenation of 1,3-butadiene over Au/ZrO_2 catalysts, Angew. Chem. Int. Ed. Engl. 44 (2005) 7132–7135, https://doi.org/10.1002/anie.200502101.
[7] G.X. Pei, X.Y. Liu, A. Wang, L. Li, Y. Huang, T. Zhang, J.W. Lee, B.W.L. Jang, C.-Y. Mou, Promotional effect of Pd single atoms on Au nanoparticles supported on silica for the selective hydrogenation of acetylene in excess ethylene, New J. Chem. 38 (2014) 2043–2051, https://doi.org/10.1039/c3nj01136d.
[8] G.X. Pei, Y. Liu, Y.Liu X, A. Wang, A.F. Lee, M.A. Isaacs, L. Li, X. Pan, X. Yang, X. Wang, Z. Tai, K. Wilson, T. Zhang, Ag alloyed Pd single-atom catalysts for efficient selective hydrogenation of acetylene to ethylene in excess ethylene, ACS Catal. 5 (2015) 3717–3725, https://doi.org/10.1021/acscatal.5b00700.

[9] P. Aich, H. Wei, B. Basan, A.J. Kropf, N.M. Schweitzer, C.L. Marshall, J.T. Miller, R. Meyer, Single-atom alloy Pd − Ag catalyst for selective hydrogenation of acrolein, J. Phys. Chem. C 119 (2015) 18140–18148, https://doi.org/10.1021/acs.jpcc.5b01357.

[10] A.J. McCue, A. Gibson, J.A. Anderson, Palladium assisted copper/alumina catalysts for the selective hydrogenation of propyne, propadiene and propene mixed feeds, Chem. Eng. J. 285 (2016) 384–391, https://doi.org/10.1016/j.cej.2015.09.118.

[11] X. Cao, Y. Ji, Y. Luo, Dehydrogenation of propane to propylene by a Pd/Cu single-atom catalyst: insight from first-principles calculations, J. Phys. Chem. C 119 (2015) 1016–1023, https://doi.org/10.1021/jp508625b.

[12] H. Zhang, K. Kawashima, M. Okumura, N. Toshima, Colloidal Au single-atom catalysts embedded on Pd nanoclusters, J. Mater. Chem. 2 (2014) 13498, https://doi.org/10.1039/c4ta01696c.

[13] X. Cheng, Y. Zhao, F. Li, Y. Liu, Catalytic mechanisms of Au11 and Au11-nPtn (n = 1–2) clusters: a DFT investigation on the oxidation of CO by O_2, J. Mol. Model. 21 (2015) 230, https://doi.org/10.1007/s00894-015-2780-4.

[14] Y. Yao, D.W. Goodman, New insights into structure–activity relationships for propane hydrogenolysis over Ni–Cu bimetallic catalysts, RSC Adv. 5 (2015) 43547–43551, https://doi.org/10.1039/c5ra07433a.

[15] L. Zhang, A. Wang, T. Miller, X. Liu, X. Yang, W. Wang, L. Li, Y. Huang, C. Mou, T. Zhang, Efficient and durable Au alloyed Pd single-atom catalyst for the Ullmann reaction of aryl chlorides in water, ACS Catal. 4 (2014) 1546–1553, https://doi.org/10.1021/cs500071c.

[16] G. Kyriakou, M.B. Boucher, A.D. Jewell, E.A. Lewis, T.J. Lawton, A.E. Baber, H.L. Tierney, M. Flytzani-Stephanopoulos, E.C.H. Sykes, Isolated metal atom geometries as a strategy for selective heterogeneous hydrogenations, Science 335 (2012) 1209–1212, https://doi.org/10.1126/science.1215864.

[17] M.B. Boucher, B. Zugic, G. Cladaras, J. Kammert, M.D. Marcinkowski, T.J. Lawton, E.C.H. Sykes, M. Flytzani-Stephanopoulos, Single atom alloy surface analogs in Pd0.18Cu15 nanoparticles for selective hydrogenation reactions, Phys. Chem. Chem. Phys. 15 (2013) 12187–12196, https://doi.org/10.1039/c3cp51538a.

[18] F.R. Lucci, J. Liu, M.D. Marcinkowski, M. Yang, L.F. Allard, M. Flytzani-Stephanopoulos, E.C.H. Sykes, Selective hydrogenation of 1,3-butadiene on platinum – copper alloys at the single-atom limit, Nat. Commun. 6 (2015) 8550, https://doi.org/10.1038/ncomms9550.

[19] J. Liu, F.R. Lucci, M. Yang, S. Lee, M.D. Marcinkowski, A.J. Therrien, C.T. Williams, E.C.H. Sykes, M. Flytzani-Stephanopoulos, Tackling CO Poisoning with Single-Atom Alloy Catalysts, J. Am. Chem. Soc. 138 (2016) 6396–6399, https://doi.org/10.1021/jacs.6b03339.

[20] J. Shan, F.R. Lucci, J. Liu, M. El-Soda, M.D. Marcinkowski, L.F. Allard, E.C.H. Sykes, M. Flytzani-Stephanopoulos, Water co-catalyzed selective dehydrogenation of methanol to formaldehyde and hydrogen, Surf. Sci. 650 (2016) 121–129 http://dx.doi.org/10.1016/j.susc.2016.02.010.

[21] P. Claus, Heterogeneously catalysed hydrogenation using gold catalysts, Appl. Catal. 291 (2005) 222–229, https://doi.org/10.1016/j.apcata.2004.12.048.

[22] L. Mcewan, M. Julius, S. Roberts, J.C.Q. Fletcher, A review of the use of gold catalysts in selective hydrogenation reactions, Gold Bull. 43 (2010) 298–306, https://doi.org/10.1007/BF03214999.

[23] M. Haruta, Size- and support-dependency in the catalysis of gold, Catal. Today 861 (1997) 153–166, https://doi.org/10.1016/S0920-5861(96)00208-8.

[24] C. Mohr, H. Hofmeister, J. Radnik, P. Claus, Identification of active sites in gold-catalyzed hydrogenation of acrolein, J. Am. Chem. Soc. 103 (2003) 178–180, https://doi.org/10.1021/ja027321q.

[25] B. Hammer, J.K. Nørskov, Why gold is the noblest of all the metals, Nature 376 (1995) 238–240.

[26] A. Wittstock, V. Zielasek, J. Biener, C.M. Friend, M. Bäumer, M. Baeumer, Nanoporous gold catalysts for selective gas-phase oxidative coupling of methanol at low temperature, Science 327 (2010) 319–322, https://doi.org/10.1126/science.1183591.

[27] M. Neurock, W.T. Tysoe, Mechanistic insights in the catalytic synthesis of vinyl acetate on palladium and gold/palladium alloy surfaces, Top. Catal. 56 (2013) 1314–1332, https://doi.org/10.1007/s11244-013-0153-8.

[28] F. Calaza, D. Stacchiola, M. Neurock, W.T. Tysoe, Coverage effects on the palladium-catalyzed synthesis of vinyl acetate: comparison between theory and experiment, J. Am. Chem. Soc. 132 (2010) 2202–2207, https://doi.org/10.1021/ja907061m.

[29] M. Chen, D. Kumar, C. Yi, D.W. Goodman, The promotional effect of gold in catalysis by palladium-gold, Science 310 (2005) 291–293, https://doi.org/10.1126/science.1115800.

[30] D.I. Enache, J.K. Edwards, P. Landon, B. Solsona-Espriu, A.F. Carley, A.A. Herzing, M. Watanabe, C.J. Kiely, D.W. Knight, G.J. Hutchings, Solvent-free oxidation of primary alcohols to aldehydes using Au-Pd/TiO2 catalysts, Science 311 (2006) 362–365, https://doi.org/10.1126/science.1120560.

[31] A.V. Beletskaya, D.A. Pichugina, A.F. Shestakov, N.E. Kuz 'menko, Formation of H2O2 on Au20 and Au19Pd clusters: understanding the structure effect on the atomic level, J. Phys. Chem. A 117 (2013) 6817–6826, https://doi.org/10.1021/jp4040437.

[32] F. Gao, Y. Wang, D.W. Goodman, CO oxidation over AuPd(100) from ultrahigh vacuum to near-atmospheric pressures: the critical role of contiguous Pd atoms, J. Am. Chem. Soc. 131 (2009) 5734–5735, https://doi.org/10.1021/ja9008437.

[33] Z. Li, F. Gao, W.T. Tysoe, Carbon monoxide oxidation over Au/Pd (100) model alloy catalysts†, J. Phys. Chem. C 114 (2010) 16909–16916, https://doi.org/10.1021/jp911374u.

[34] W.-Y. Yu, L. Zhang, G.M. Mullen, G. Henkelman, C.B. Mullins, Oxygen activation and reaction on Pd–Au bimetallic surfaces, J. Phys. Chem. C 119 (2015) 11754–11762, https://doi.org/10.1021/acs.jpcc.5b02970.

[35] N. Saliba, D.. Parker, B.. Koel, Adsorption of oxygen on Au(111) by exposure to ozone, Surf. Sci. 410 (1998) 270–282, https://doi.org/10.1016/S0039-6028(98)00309-4.

[36] B. Xu, J. Haubrich, C.G. Freyschlag, R.J. Madix, C.M. Friend, Oxygen-assisted cross-coupling of methanol with alkyl alcohols on metallic gold, Chem. Sci. 1 (2010) 310, https://doi.org/10.1039/c0sc00214c.

[37] B. Xu, R.J. Madix, C.M. Friend, Achieving optimum selectivity in oxygen assisted alcohol cross-coupling on gold, J. Am. Chem. Soc. 132 (2010) 16571–16580, https://doi.org/10.1021/ja106706v.

[38] X. Liu, B. Xu, J. Haubrich, R.J. Madix, C.M. Friend, Surface-mediated self-coupling of ethanol on gold, J. Am. Chem. Soc. 131 (2009) 5757–5759, https://doi.org/10.1021/ja900822r.

[39] H.L. Tierney, A.E. Baber, J.R. Kitchin, E. Charles, H. Sykes, Hydrogen dissociation and spillover on individual isolated palladium atoms, Phys. Rev. Lett. (n.d.). doi:10.1103/PhysRevLett.103.246102.

[40] G. Kresse, J. Furthmüller, Efficiency of ab-initio total energy calculations for metals and semiconductors using a plane-wave basis set, Comput. Mater. Sci. 6 (1996) 15–50, https://doi.org/10.1016/0927-0256(96)00008-0.

[41] G. Kresse, Dissociation and sticking of H_2 on the Ni(111), (100), and (110) substrate, Phys. Rev. B 62 (2000) 8295–8305, https://doi.org/10.1103/PhysRevB.62.8295.

[42] P.E. Blöchl, Projector augmented-wave method, Phys. Rev. B 50 (1994) 17953–17979, https://doi.org/10.1103/PhysRevB.50.17953.

[43] G. Kresse, D. Joubert, From ultrasoft pseudopotentials to the projector augmented-wave method, Phys. Rev. B 59 (1999) 1758–1775, https://doi.org/10.1103/physrevb.59.1758.

[44] J.P. Perdew, K. Burke, M. Ernzerhof, Generalized gradient approximation made simple, Phys. Rev. Lett. 77 (1996) 3865–3868, https://doi.org/10.1103/PhysRevLett.77.3865.

[45] G. Henkelman, B.P. Uberuaga, H. Jónsson, A climbing image nudged elastic band method for finding saddle points and minimum energy paths, J. Chem. Phys. 113 (2000) 9901–9904, https://doi.org/10.1063/1.1329672.

[46] G. Henkelman, H. Jónsson, Improved tangent estimate in the nudged elastic band method for finding minimum energy paths and saddle points, J. Chem. Phys. 113 (2000) 9978–9985, https://doi.org/10.1063/1.1323224.

[47] H. Monkhorst, J. Pack, Special points for Brillouin zone integrations, Phys. Rev. B 13 (1976) 5188–5192, https://doi.org/10.1103/PhysRevB.13.5188.

[48] A.E. Baber, H.L. Tierney, E.C.H. Sykes, Atomic-scale geometry and electronic structure of catalytically important Pd/Au alloys, ACS Nano 4 (2010) 1637–1645, https://doi.org/10.1021/nn901390y.

[49] M. Ruff, N. Takehiro, P. Liu, J.K. Nørskov, R.J. Behm, Size-specific chemistry on bimetallic surfaces: A combined experimental and theoretical study, Chem. Phys. Chem. 8 (2007) 2068–2071, https://doi.org/10.1002/cphc.200700070.

[50] F. Maroun, F. Ozanam, O.M. Magnussen, R.J. Behm, The role of atomic ensembles in the reactivity of bimetallic electrocatalysts, Science 293 (2001) 1811–1814, https://doi.org/10.1126/science.1061696.

[51] C. Casari, S. Foglio, F. Siviero, A. Li Bassi, M. Passoni, C. Bottani, Direct observation of the basic mechanisms of Pd island nucleation on Au(111), Phys. Rev. B 79 (2009) 1–9, https://doi.org/10.1103/PhysRevB.79.195402.

[52] J.V. Barth, H. Brune, G. Ertl, R.J. Behm, Scanning tunneling microscopy observations on the reconstructed Au(111) surface: atomic structure, long-range superstructure, rotational domains, and surface defects, Phys. Rev. B 42 (1990) 9307–9318, https://doi.org/10.1103/PhysRevB.42.9307.

[53] J.A. Meyer, I.D. Baikie, E. Kopatzki, R.J. Behm, Preferential island nucleation at the elbows of the Au(111) herringbone reconstruction through place exchange, Surf. Sci. 365 (1996) L647–L651, https://doi.org/10.1016/0039-6028(96)00852-7.

[54] S. Venkatachalam, T. Jacob, Hydrogen adsorption on Pd-containing Au(111) bimetallic surfaces, PCCP 11 (2009) 3010, https://doi.org/10.1039/b905911n.

[55] I.V Yudanov, K.M. Neyman, Stabilization of Au at edges of bimetallic PdAu nanocrystallites, Phys. Chem. Chem. Phys. 12 (2010) 5094–5100, https://doi.org/10.1039/b927048e.

[56] D. Yuan, X. Gong, R. Wu, Atomic configurations of Pd atoms in PdAu(111) bimetallic surfaces investigated using the first-principles pseudopotential plane wave approach, Phys. Rev. B 75 (2007) 085428, , https://doi.org/10.1103/PhysRevB.75.085428.

[57] F.R. Lucci, M.T. Darby, M.F.G. Mattera, C.J. Ivimey, A.J. Therrien, A. Michaelides, M. Stamatakis, E.C.H. Sykes, Controlling hydrogen activation, spillover, and desorption with Pd-Au single atom alloys, J. Phys. Chem. Lett. 7 (2016) 480–485, https://doi.org/10.1021/acs.jpclett.5b02400.

[58] N. Saliba, D.H. Parker, B.E. Koel, Adsorption of oxygen on Au(111) by exposure to ozone, Surf. Sci. 410 (1998) 270–282.

[59] B.K. Min, A.R. Alemozafar, D. Pinnaduwage, X. Deng, C.M. Friend, Efficient CO oxidation at low temperature on Au(111), J. Phys. Chem. B 110 (2006) 19833–19838, https://doi.org/10.1021/jp0616213.

[60] X. Deng, B.K. Min, A. Guloy, C.M. Friend, Enhancement of O2 dissociation on Au (111) by adsorbed oxygen: Implications for oxidation catalysis, J. Am. Chem. Soc. 127 (2005) 9267–9270, https://doi.org/10.1021/ja050144j.

[61] T. Thuening, J. Walker, H. Adams, O. Furlong, W.T. Tysoe, Kinetics of low-temperature CO oxidation on Au(111), Surf. Sci. 648 (2016) 236–241, https://doi.org/10.1016/j.susc.2015.12.010.

[62] K.A. Davis, D.W. Goodman, Propene adsorption on clean and oxygen-covered Au (111) and Au(100) surfaces, J. Phys. Chem. B 104 (2000) 8557–8562, https://doi.org/10.1021/jp001699y.

[63] A.E. Baber, D. Torres, K. Müller, M. Nazzarro, P. Liu, D.E. Starr, D.J. Stacchiola, Reactivity and morphology of oxygen-modified Au surfaces, J. Phys. Chem. C 116 (2012) 18292–18299, https://doi.org/10.1021/jp3056653.

[64] F. Hiebel, M.M. Montemore, E. Kaxiras, C.M. Friend, Direct visualization of quasi-ordered oxygen chain structures on Au(110)-(1 × 2), Surf. Sci. 650 (2015) 5–10, https://doi.org/10.1016/j.susc.2015.09.018.